

Investigation of minority carrier trapping in *n*-type doped ZnSe using photoluminescence decay measurements

J. S. Massa, G. S. Buller, A. C. Walker, J. Simpson,^{a)} K. A. Prior, and B. C. Cavenett
Department of Physics, Heriot-Watt University, Riccarton, Edinburgh, EH14 4AS, United Kingdom

(Received 31 January 1995; accepted for publication 14 April 1995)

Temperature dependent photoluminescence decay measurements have been used to study the minority carrier dynamics in iodine-doped ZnSe grown by molecular beam epitaxy. The existence of three deep acceptor levels with energies at 80, 120, and 350 meV above the valence band has been established. The 80 and 120 meV levels have a density dependence directly related to the iodine doping density whilst the level at 350 meV does not. Significant broadband donor-acceptor emission is observed from this material and appears to be associated with the acceptor level at 350 meV. © 1995 American Institute of Physics.

The optoelectronic properties of II-VI semiconductors and in particular ZnSe, are of considerable interest at present due to the recent fabrication of photonic devices operating in the blue/blue-green spectral region.¹⁻⁵ The performance of these devices can be greatly influenced by the presence of impurities and lattice defects in the material, since these can act as traps or centers for nonradiative recombination and thus deplete the free-carrier concentration. The nature and origin of these centers is of crucial importance for growth optimization and hence improvement of device performance in the future. Electrical techniques such as deep-level transient spectroscopy (DLTS) have been routinely used to study majority carrier trapping centers in both *n*- and *p*-type doped ZnSe.⁶⁻⁹ However, investigation of minority carrier trapping has been more limited^{10,11} with the need to use optical DLTS (ODLTS) for the commonly used Schottky diode structures.

In a recent publication¹² we reported a room temperature, time-resolved photoluminescence (TRPL) study, of device quality, *n*-type (iodine-doped) and *p*-type (nitrogen-doped) ZnSe grown by molecular beam epitaxy (MBE). For *n*-type material, under low injection level conditions, the decay rate of the band-edge photoluminescence (PL) increased with increasing sample doping density. The PL decays had an approximately exponential form, consistent with a linear recombination process. For the more heavily doped *n*-type samples, additional broadband emission was observed over the spectral region 500–700 nm. This emission decayed on a microsecond time scale and was nonexponential, corresponding to a nonlinear recombination process. It was concluded that the dominant recombination mechanism for *n*-type material was via minority carrier capture by deep-level acceptors, followed by radiative donor-acceptor recombination. In this letter, the study of *n*-type material has been extended to include variable temperature measurements and a greater range of sample doping densities.

The instrument used to perform the measurements in this study is microscope-based (a derivative of an Edinburgh Instruments Life-Map) and has been described elsewhere.¹³ Sample excitation was provided at a wavelength of 420 nm,

by a commercial frequency doubled picosecond AlGaAs laser diode (pulse duration <20 ps). The detector was an actively quenched silicon single-photon avalanche diode (SPAD)¹⁴ with an active area $\sim 7 \mu\text{m}$ diameter. Using appropriate imaging and polarization optics, TRPL measurements can be performed with a spatial resolution of $<5 \mu\text{m}$ (Ref. 15) and over a spectral range 430–1100 nm. The instrument uses the time-correlated single photon counting technique¹⁶ and has an instrumental full width at half-maximum (FWHM) of ~ 50 ps.

The samples under investigation were MBE-grown ZnSe layers of $\sim 2 \mu\text{m}$ thickness, grown on a semi-insulating GaAs substrate, [100] orientation. The samples, were either nominally undoped, i.e., with an uncompensated donor concentration, $N_D - N_A, < 10^{16} \text{ cm}^{-3}$, or iodine (*n*-type) doped with various values of $N_D - N_A$ ranging up to $2 \times 10^{19} \text{ cm}^{-3}$. $N_D - N_A$ was measured using electrochemical capacitance-voltage profiling,¹⁷ and was found to be uniform in the direction of growth.

The samples were mounted under the microscope objective within a continuous flow helium cryostat (Oxford Instruments CF1104) which had been modified to allow close optical access to the sample. The laser excitation and PL collection were accomplished using a long working distance (~ 8 mm) reflecting objective (Ealing $\times 36$), which led to a reduction in PL collection efficiency of $\sim 30\%$ compared to the refracting objective configuration used for room temperature measurements. In all the measurements presented in this letter, the excitation pulse energy incident on the sample was ~ 20 fJ and was focused to an elliptical spot of area $\sim 40 \mu\text{m}^2$. Assuming an absorption coefficient of $\sim 10^5 \text{ cm}^{-1}$ (Ref. 18) this yielded a peak photogenerated carrier density of $< 10^{16} \text{ cm}^{-3}$.

The room temperature steady state PL spectra for the iodine doped samples shows a single feature at ~ 440 – 450 nm together with the much broader deep level emission in the 500–700 nm region. The spectrally integrated intensity ratio of near band edge to deep level emission is $\sim 1:2.5$ for the $1.5 \times 10^{18} \text{ cm}^{-3}$ doped material and $\sim 1.5:1$ for the $1.3 \times 10^{17} \text{ cm}^{-3}$ doped material. Figure 1 shows the PL decays integrated over the spectral range 440–450 nm, from the $1.5 \times 10^{18} \text{ cm}^{-3}$ doped material at various temperatures between 100 and 190 K. Below 100 K the form of the decay is

^{a)}Present address: Defence Research Agency, Malvern, Worcester WR14 3PS, UK.

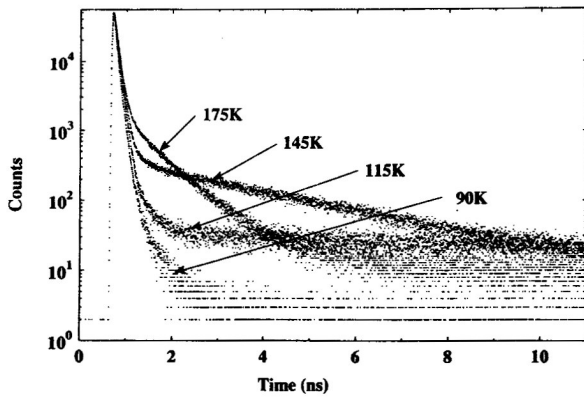


FIG. 1. PL decays from the sample with $N_D-N_A \sim 1.5 \times 10^{18} \text{ cm}^{-3}$ for temperatures in the range 100–190 K. Sample excitation was at a wavelength of 420 nm and PL detection was over the spectral range 445–455 nm. The peak photogenerated carrier density was $< 10^{16} \text{ cm}^{-3}$.

temperature invariant and follows a single exponential over more than three decades in PL intensity, with a time constant τ_1 of $\sim 20\text{--}30$ ps. At ~ 100 K, a much longer, single exponential component appears with a decay time τ_2 , > 50 ns. As the temperature is increased, this component becomes progressively more rapid, and larger in amplitude, before merging into the main PL decay at a temperature of ~ 190 K. This cycle is repeated again in the temperature range $\sim 160\text{--}250$ K, and a third time in the range $360\text{--}500$ K. Similar temperature dependent behavior was observed with the $1.3 \times 10^{17} \text{ cm}^{-3}$ doped material but the initial decay rate was slower ($\tau_1 \sim 60$ ps), and the amplitude of the longer lifetime component was considerably reduced compared to the main decay. For the heavily doped material, $N_D-N_A > 10^{19} \text{ cm}^{-3}$, and the lightly doped material, $N_D-N_A < 10^{16} \text{ cm}^{-3}$, the luminescence efficiency was too low to observe the longer component above the background noise level.

The temperature dependent decays are characteristic of carrier reemission from deep trapping levels. The time constant τ_2 for such a process depends on the temperature T according to the equation¹⁹

$$\tau_2 = \frac{1}{N_B \nu \sigma} \exp(\Delta E/kT), \quad (1)$$

where ΔE and σ are the activation energy and cross section of the trap, and ν is the carrier thermal velocity. N_B is an effective density of states in the band to which the traps are coupled and is given by $N_B = (2\pi m^* kT/h^2)^{3/2}$, where $m^* = 0.6m_0$ (Ref. 4) was used for the valence band. Since the re-emission from a particular trapping level occurs over a specific temperature range the carrier dynamics can be treated separately for each level and thus, for a limited temperature range, the system can be described by three coupled rate equations consisting of the conduction and valence bands and the one, relevant, trapping level. For the doped samples, this can be further simplified to leave two equations since the injected carrier density is much less than the background carrier density, and thus the concentration of electrons in the conduction band n is effectively constant. This

also implies that the trapping and re-emission process is due to minority carriers, and thus the rate equations for the free hole and trapped hole populations, p and m , respectively, become

$$\frac{dp}{dt} = \frac{m}{\tau_2} - (Bn + b + \sigma \nu N_T)p, \quad (2)$$

$$\frac{dm}{dt} = \sigma \nu N_T p - \frac{m}{\tau_2}, \quad (3)$$

where N_T is the trap density. B is the radiative recombination coefficient and b is the rate at which carriers are trapped by other levels, not involved in the re-emission process. The PL decays for samples with $N_D-N_A \sim 1.3 \times 10^{17} \text{ cm}^{-3}$, and $N_D-N_A \sim 1.5 \times 10^{18} \text{ cm}^{-3}$ were fitted to the above model by solving the rate equations numerically and using reconvolution analysis with three adjustable parameters τ_2 , $\sigma \nu N_T$, and $(Bn + b)$. The model assumes that the trapping and recombination processes are linear, i.e., that the traps are not saturated, and this is confirmed by the resulting best fit parameters which were consistent over each temperature range. Figure 2 shows plots of the deduced τ_2 values versus $1000/T$ for the three different trapping levels. Since N_B and ν are also temperature dependent the data in Fig. 2 was fitted to Eq. (1) using a nonlinear least squares fit and the resulting activation energies and cross sections are given in Table I. Also shown in Table I are the densities of each trap in the two samples, obtained from the best fit parameters to the model. It should be noted that TRPL can measure reemission rates which are $\sim 4\text{--}5$ orders of magnitude higher than DLTS and other similar techniques, and thus it is possible to study much shallower levels using this method.

As previously mentioned, for the more heavily doped samples $N_D-N_A > 10^{17} \text{ cm}^{-3}$, considerable deep level emission was observed in the 500–700 nm spectral region. Since the decay of this luminescence was nonexponential, as would be expected for recombination in the minority carrier regime, it was attributed to donor–acceptor pair (DAP) recombination in previous work.¹² In the temperature range 300–500 K the intensity of the DAP emission is greatly re-

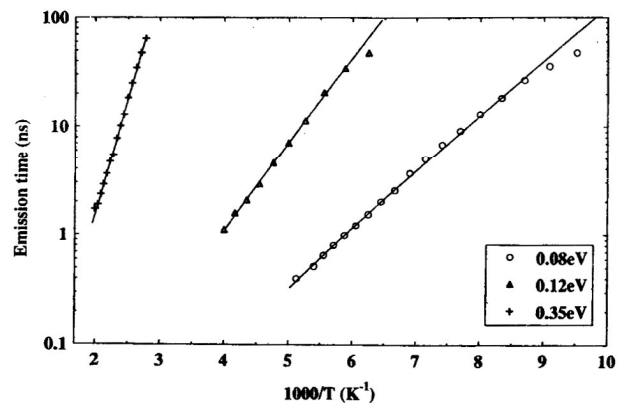


FIG. 2. Arrhenius plots for the three acceptor levels observed in iodine doped ZnSe. The data shown were obtained from the temperature dependence of the re-emission in the sample with $N_D-N_A \sim 1.5 \times 10^{18} \text{ cm}^{-3}$. The activation energies were obtained from nonlinear least-squares fit to Eq. (1), shown by the solid lines through the data.

TABLE I. Trap parameters for the three acceptor levels A_1 , A_2 , and A_3 observed in iodine doped ZnSe.

	A_1	A_2	A_3
ΔE (eV)	0.08	0.12	0.35
σ (cm ⁻²)	9.5×10^{-15}	4.6×10^{-15}	8.6×10^{-15}
N_T (cm ⁻³)			
Sample:			
$N_D - N_A \sim 1.3 \times 10^{17}$ cm ⁻³	2.1×10^{15}	6.9×10^{14}	4.9×10^{15}
$N_D - N_A \sim 1.5 \times 10^{18}$ cm ⁻³	3.2×10^{16}	7.2×10^{15}	1.4×10^{16}

duced with increasing temperature and the decay rate of the DAP emission increases significantly. The temperature variation of the initial decay time constant shows the same trend as the reemission time constant (τ_2) associated with acceptor level A_3 . It thus seems likely that the acceptor level at 350 meV above the valence band (A_3) is involved in the DAP emission process and that the decrease in DAP emission at these temperatures is due to the reemission of trapped holes into the valence band from this level. However, the luminescence intensity around the band edge wavelength also decreases as the temperature is raised above 300 K, and thus nonradiative recombination from the valence band must also be of increasing importance.

For the three levels indicated in Table I, both A_1 and A_2 appear to increase proportionately with doping density whilst A_3 is much more weakly dependent. Since the concentrations of A_1 and A_2 are $\sim 2\%$ of $N_D - N_A$ it seems likely that these levels are either due to impurities introduced with the iodine or defects associated with the iodine. Leigh *et al.*¹¹ observed acceptor levels at 85 and 100 meV in nitrogen doped material using ODLTS, and a level at ~ 110 meV is commonly attributed to a hydrogenic acceptor. The level A_3 at 350 meV does not appear to have been observed previously but is probably due to a lattice defect such as a zinc vacancy or an associated complex. Its presence could not be confirmed in the lightly doped samples due to the low luminescence efficiency of this material. The spectral width of the deep level emission (500–700 nm) would seem to indicate a strong lattice coupling for this level.

In conclusion, PL decay time measurements have been used to study the minority carrier dynamics in iodine doped ZnSe grown by MBE. The presence of three deep acceptor levels has been established, with energies of around 80, 120, and 350 meV above the valence band. The 80 and 120 meV levels appear to be directly related to the iodine dopant and are possibly due to an elemental impurity or a dopant related defect. The 350 meV level is likely responsible for the strong DAP emission from this material and is probably associated

with a lattice defect since its concentration does not increase proportionately with the doping density.

The authors acknowledge the support of the Royal Society Paul Instrument Fund and the UK Science and Engineering Research Council (SERC). J.S.M. was supported by a SERC CASE studentship with Edinburgh Instruments Ltd. The actively quenched SPADs are used by agreement of Professor Sergio Cova and co-workers, Polytechnico di Milano, Italy.

- ¹ J. Ren, K. A. Bowers, B. Sneed, D. L. Dreifus, J. W. Cook, J. F. Schetzina, and R. M. Kolbas, *Appl. Phys. Lett.* **57**, 1901 (1990).
- ² M. A. Haase, J. Qiu, J. M. DePuydt, and H. Cheng, *Appl. Phys. Lett.* **59**, 1272 (1991).
- ³ H. Jeon, J. Ding, W. Patterson, A. U. Nurmikko, W. Xie, D. C. Grillo, M. Kobayashi, and R. L. Gunshor, *Appl. Phys. Lett.* **59**, 3619 (1991).
- ⁴ S. Y. Wang, Y. Kawakami, J. Simpson, H. Stewart, K. A. Prior, and B. C. Cavenett, *Appl. Phys. Lett.* **62**, 1715 (1993).
- ⁵ S. Y. Wang, G. Horsburgh, P. Thompson, I. Hauksson, J. T. Mullins, K. A. Prior, and B. C. Cavenett, *Appl. Phys. Lett.* **63**, 857 (1993).
- ⁶ Y. H. Wang and S. S. Li, *J. Appl. Phys.* **68**, 2535 (1990).
- ⁷ K. Ando, Y. Kawaguchi, T. Ohno, A. Ohki, and S. Zembutsu, *Appl. Phys. Lett.* **63**, 191 (1993).
- ⁸ B. Hu, G. Karczewski, H. Luo, N. Samarth, and J. K. Furdyna, *Appl. Phys. Lett.* **63**, 358 (1993).
- ⁹ G. Karczewski, B. Hu, A. Yin, H. Luo, and J. K. Furdyna, *J. Appl. Phys.* **75**, 7382 (1994).
- ¹⁰ K. A. Christianson and B. W. Wessels, *J. Appl. Phys.* **54**, 4205 (1983).
- ¹¹ W. B. Leigh and B. W. Wessels, *J. Appl. Phys.* **55**, 1614 (1984).
- ¹² J. S. Massa, G. S. Buller, A. C. Walker, J. Simpson, K. A. Prior, and B. C. Cavenett, *Appl. Phys. Lett.* **64**, 589 (1994).
- ¹³ G. S. Buller, J. S. Massa, and A. C. Walker, *Rev. Sci. Instrum.* **63**, 2994 (1992).
- ¹⁴ A. Lacaite, M. Ghioni, and S. Cova, *Electron. Lett.* **25**, 841 (1989).
- ¹⁵ J. S. Massa, G. S. Buller, A. C. Walker, J. L. Oudar, E. V. K. Rao, B. G. Sfez, and R. Kuselewicz, *Appl. Phys. Lett.* **61**, 2205 (1992).
- ¹⁶ D. V. O'Connor and D. Phillips, *Time-Correlated Single Photon Counting* (Academic, New York, 1983).
- ¹⁷ S. Y. Wang, J. Simpson, K. A. Prior, and B. C. Cavenett, *J. Appl. Phys.* **72**, 5311 (1992).
- ¹⁸ S. Adachi and T. Taguchi, *Phys. Rev. B* **43**, 9569 (1991).
- ¹⁹ See for example, R. H. Bube, *Photoconductivity in Solids* (Wiley, New York, 1960).